Design of photovoltaic MPPT based charger for lead-acid batteries

Subhransu Padhee, Umesh Chandra Pati, Kamalakanta Mahapatra
Department of Electronics and Communication Engineering
National Institute of Technology
Rourkela, Odisha, India
subhransupadhee@gmail.com, ucpati@nitrkl.ac.in, kkm@nitrkl.ac.in

Abstract— **An energy storage system plays an important role in the operation of micro-grid and electric vehicle. Battery management system (BMS) in micro-grid and electric vehicle is one of the challenging areas and has witnessed much research interest. This paper provides the design and implementation details of photovoltaic (PV) based charger for lead-acid batteries. For charging the battery, a synchronous buck converter is used which is fed by a PV panel. Maximum power point tracking (MPPT) algorithm extracts maximum power from the PV panel and charges the battery through the DC-DC converter. The battery is charged both in float charge mode and bulk charge mode. Modeling and simulation of PV based battery charger is provided in this paper.**

Keywords—Battery Management System; PV charger; Lead-acid battery; MPPT; DC-DC Converter

I. INTRODUCTION

Renewable energy sources such as photovoltaic, wind energy and fuel cell have been used for past few years to meet the huge demand of energy. The output voltage of photovoltaic (PV) panel varies with change in meteorological and environmental conditions such as change in solar irradiance and change in ambient temperature. PV based application can be used either in stand-alone mode or in grid-tied mode or can also can be used along with other renewable energy sources for hybrid generation mode. In all of the cases, the provision of a battery is necessary. In grid-tied mode, battery can deliver stored energy or absorb surplus energy. In standalone application, the battery provides necessary power during peak and non-peak time. There are different types of rechargeable batteries such as lead-acid battery, Li-ion battery, Ni-Cd battery and NiMH battery etc. Lead-acid battery is one of the oldest rechargeable batteries which is widely used because it is efficient and is of low cost. Other salient features of lead-acid battery are that it is tolerant to overcharge, can deliver high current and has low impedance.

Battery management system (BMS) is one of the most important aspects of micro-grid system. BMS is responsible to monitor charging, discharging, state of charge and other important aspect of the battery. Charging of battery is one of the critical functions of BMS. PV chargers are used to charge the battery when sun light is incident upon the PV panel. The charger must charge the battery to its optimum level and terminate the charge when the battery is fully charged. The PV based charger finds widespread applications in portable electronics, electric vehicle and backup power unit.

A classical review of different battery charger topology used in plug-in electric and hybrid electric vehicle is reported in [1]. When voltage supplied by PV panel is greater than the required battery voltage, a step down DC-DC converter is used. Off-line battery charger based on buck-boost power factor correction converter has been reported in [2]. Chiang et.al [3], used SEPIC converter to design a PV charger. Though SEPIC converter is not as efficient as other type of converter, it has easy to drive switch and low input current ripple. A low cost roof-top solar charger is developed in [4], which uses buck converter and reduced number of sensors to implement the solar charger.

This paper provides a comprehensive design and implementation details of solar photovoltaic charger for lead-acid battery using a synchronous buck converter. For the PV charger, perturb and observe MPPT algorithm is used. The battery is charged both in bulk mode and float charging mode.

This paper is organized as follows: Section II provides a detailed problem formulation. Section III presents the mathematical model of photovoltaic system and MPPT. Section IV provides detailed mathematical model of lead-acid battery. Modeling of DC-DC synchronous buck converter is discussed in section V. Section VI presents the simulation results. Section VII provides concluding remarks to the paper.

II. PROBLEM FORMULATION

The schematic diagram of PV based battery charger is shown in Fig. 1. A PV panel is used as the energy source which produces electrical output. The electrical power generated by the PV panel varies with varying solar irradiance and ambient temperature. A lead-acid battery (12V, 18AH) is used to store the charge. DC-DC synchronous buck converter is used to charge the battery to its optimal level with PV panel as the input source.

978-1-5090-0706-6/16/$31.00 ©2016 IEEE

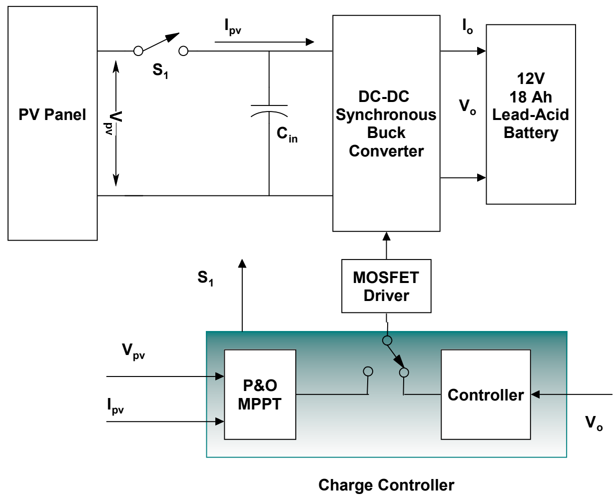

Fig. 1. Block diagram of photovoltaic based battery charger unit

The PV based battery charger operates in two different modes, i.e. bulk charge mode and float chagre mode. In bulk charge mode the perturb and observe MPPT works and in float charge mode, the controller operates to maintain the optimal voltage level of the battery. When the solar power is greater than 5 Watt, then the battery is charged in bulk mode using MPPT technique. When the battery voltage is equal to maximum battery voltage, the battery is charged in float charge mode. An additional switch (S_1) is provided to cut-off the supply from the PV panel to the battery. In this PV based charger, two voltage sensors are used and one current sensor is used. The voltage sensors are used to measure PV voltage and battery voltage respectively whereas the current sensor is used to measure the current of PV panel. A MOSFET driver circuit is used to provide required gate pulses to the MOSFET of the DC-DC synchronous buck converter. The synchronous buck converter is preferred over buck converter due to its improved efficiency.

III. PHOTOVOLTAIC SYSTEM

A reliable electrical model of photovoltaic cell is essential to design a photovoltaic application. Various electrical equivalent model of PV cell are developed in literature. Some of the well-known models are practical model, simplified series model, idea model, double diode model and triple diode model [5]. Practical PV cell constitutes of a voltage dependent current source, diode, series resistance R_s and parallel resistance R_p. The typical electrical equivalent model of practical PV cell is illustrated in Fig. 2.

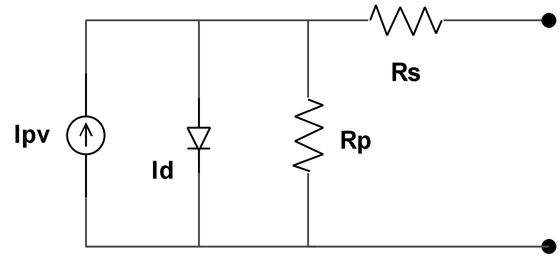

Fig. 2. Typical electrical equivalent model of PV cell

Current of the above mentioned circuit is represented as

$$I = I_{pv} - I_d \qquad (1)$$

Here I_{pv} is current of PV cell and I_d represents Shockley diode equation which can be represented as

$$I_d = I_o \left[\exp\left(\frac{qV}{akT} \right) - 1 \right] \qquad (2)$$

Substituting eq(2) in eq(1), the current can be represented as

$$I = I_{pv} - I_o \left[\exp\left(\frac{qV}{akT} \right) - 1 \right] \qquad (3)$$

Here I_o represents the leakage current of diode, q represents the electron charge (1.6x10^{-19} Coulomb), K represents Boltzmann constant (1.38x10^{-23} m^2 Kg s^{-2} K^{-1}), a represents the diode ideality factor and T represents temperature. Considering series and parallel resistance as shown in Fig. 1, Eq(3) can be re-written as

$$I = I_{pv} - I_o \left[\exp\left(\frac{V + R_s I}{V_t a} \right) - 1 \right] - \frac{V + R_s I}{R_p} \qquad (4)$$

Here, the thermal voltage of PV cell can be represented as

$$V_t = \frac{N_s KT}{q}$$

The current of solar cell depends on different environmental and meteorological parameters. The output voltage of solar cell is varies with change in ambient temperature.

$$I_{pv} = \left(I_{pv,n} + K_I \Delta_T \right) \left(\frac{G}{G_n} \right) \qquad (5)$$

Here, $I_{pv,n}$ is the light generated current at nominal operating condition (25°C, 1000 W/m^2), Δ_T is the difference of temperature, G is the irradiance of surface, G_n is the nominal irradiance.

Increase in temperature, increases the band gap of semiconductor material and open circuit voltage and saturation current of PV cell varies according to the change in temperature. The effect of temperature on PV cell can be represented as

$$I_o = I_{o,n}\left(\frac{T_n}{T}\right)^3 \exp\left[\frac{qE_g}{ak}\left(\frac{1}{T_n}-\frac{1}{T}\right)\right] \tag{6}$$

Here, E_g is the band gap energy (1.3 eV for Si based PV cell)

The nominal saturation current can be expressed as

$$I_{o,n} = \frac{I_{sc,n}}{\exp\left(\frac{V_{oc,n}}{aV_{t,n}}\right)-1} \tag{7}$$

Eq(7) can be modified as

$$I_{o,n} = \frac{I_{sc,n}+K_V\Delta_T}{\exp\left(\frac{V_{oc,n}+K_I\Delta_T}{aV_t}\right)-1} \tag{8}$$

A. Maximum Power Point Tracking Algorithm

MPPT technique extracts the maximum possible power output from PV panel or module under any climatic conditions. Various MPPT algorithms were discussed in literature [6-7]. Some of the well-known MPPT techniques are perturb and observe [8], incremental conductance [9] and fuzzy based MPPT [10]. From these MPPT algorithms, Perturb and Observe (P&O) MPPT is widely used because this technique is not dependent on any PV panel. The hardware implementation of the said MPPT algorithm can be carried out using analog circuit as well as digital circuits. Fig. 3 illustrates the algorithm of (P&O) MPPT.

P&O MPPT checks the $\frac{dP}{dV}$ slope to determine the necessary duty cycle. The logic of P&O MPPT can be described as

$$\frac{dP}{dV} = \begin{cases} >0 & V < V_{mpp} \\ =0 & V = V_{mpp} \\ <0 & V > V_{mpp} \end{cases} \tag{9}$$

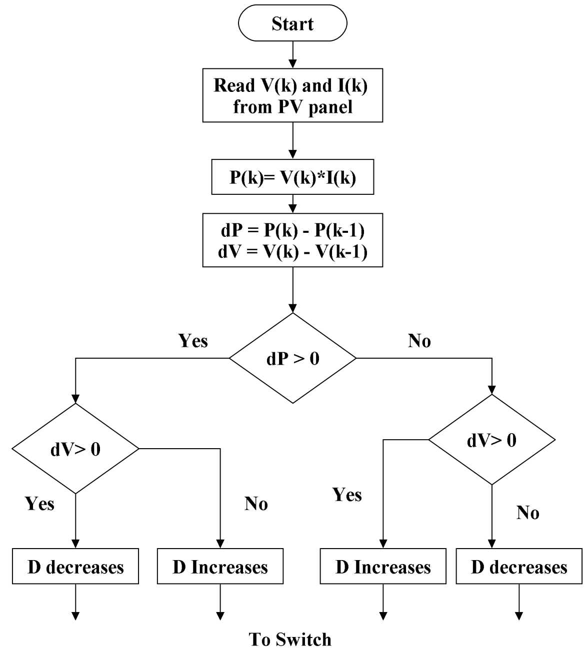

Fig. 3. Algorithm of perturb and observe maximum power point tracking

IV. MATHEMATICAL MODEL OF BATTERY

Different researchers provided mathematical model of lead acid batteries [11,12]. The electrical equivalent circuit diagram of lead-acid battery is illustrated in Fig. 4. In this electrical equivalent model the battery EMF is denoted by the voltage across the capacitor C_b. During charging the current flows through R_{bc} and R_{ovc}. During discharge, the current flows through R_{ovd} and R_{bd}.

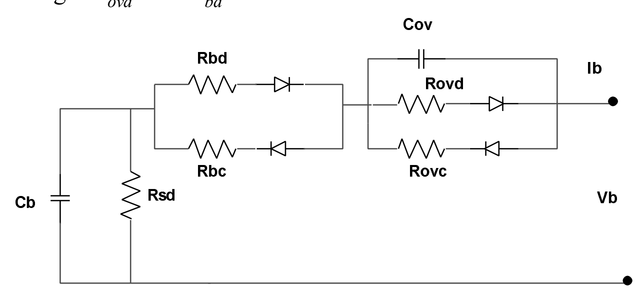

Fig. 4. Equivalent circuit diagram of lead acid battery

To quantify the behavior of battery different parameters are studied. Some of the parameters are capacity C_p and state of charge SoC

Capacity of the battery can be represented as

$$C_p = I^k t \tag{10}$$

Here, C_p is capacity of battery, I is the discharge current and t is the time of discharge

State of charge (SoC) of battery can be represented as

$$SoC = SoC_o + \frac{1}{C_n}\int_0^t I d\tau \qquad (11)$$

Here, SoC_o is initial state of charge, C_n is nominal capacitance, I is the battery current

V. Synchronous Buck Converter

Synchronous buck converter is a DC-DC converter which steps down the unregulated input voltage to a required voltage which is less than the input voltage. In this paper, the synchronous buck converter operates in continuous conduction mode (CCM). Fig. 5 represents the power circuit of synchronous buck converter.

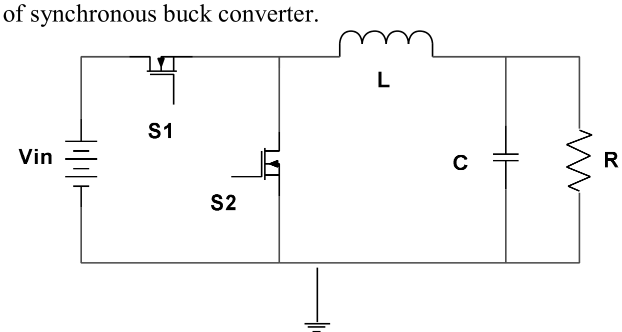

Fig. 5. Circuit diagram of synchronous buck converter

The state space model of synchronous buck converter can be represented as $\frac{dx}{dt} = Ax + Bu + D$ (12)

Here

$$A = \begin{pmatrix} 0 & 1 \\ -\frac{1}{LC} & -\frac{1}{RC} \end{pmatrix} \; B = \begin{pmatrix} 0 \\ \frac{-1}{LC} \end{pmatrix} \; D = \begin{pmatrix} 0 \\ \frac{V_{ref}}{LC} \end{pmatrix}$$

$$x = \begin{pmatrix} x_1 \\ x_2 \end{pmatrix} = \begin{pmatrix} I_L \\ V_c \end{pmatrix} \; u = V_{in}$$

The peak to peak inductor current (ΔI_L) and peak to peak ripple voltage of capacitor (ΔV_c) can be found out from the following equations

$$\Delta I_L = \frac{V_{in} D(1-D)}{f_{sw} L} \qquad (13)$$

$$\Delta V_c = \frac{V_{in} D(1-D)}{8LCf_{sw}^2} \qquad (14)$$

This paper assumes peak to peak inductor ripple (ΔI_L) and peak ripple voltage of capacitor (ΔV_c) as 5%. Here D is the duty ratio; V_{in} is the input voltage; f_{sw} is the switching frequency; L is the inductor of synchronous buck converter; C is the capacitor of synchronous buck converter

VI. Simulation Results

The power characteristics of photovoltaic module are nonlinear in nature which varies with varying environmental and meteorological conditions. This section provides MATLAB-Simulink based simulation results for PV based battery charger application.

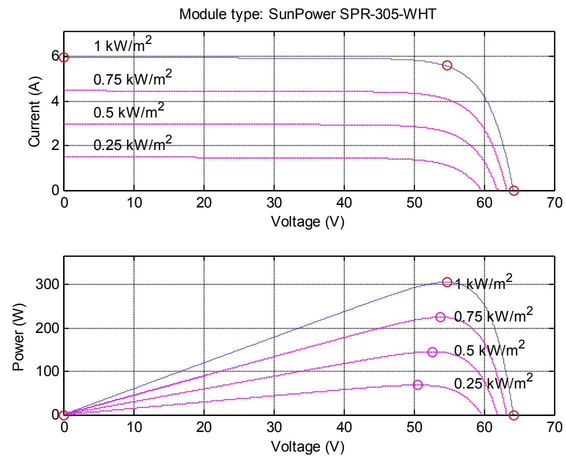

Fig. 6. P-V characteristics of PV cell with varing solar irradiance

Fig. 6 represents the P-V and V-I characteristics of PV module for varying level of solar irradiance. This paper considers SunPower made SPR-305-WHT PV module of 300W power rating. The specification of the PV module is summarized in Table I. The solar irradiance is varied from 200 W/m^2 to 1000 W/m^2 in step size of 200 and the power and current of the cell is noted.

TABLE I. Specification of SPR-305-WHT PV Panel

Parameters	Symbol	Values
Power rating at STC	P_{STC}	305 W
Power per unit area STC		187 W/m^2
Maximum voltage	V_{mp}	54.7 V
Maximum current	I_{mp}	5.58 A
Open circuit voltage	V_{oc}	64.2 V
Short circuit current	I_{sc}	5.96 A
Maximum power Temperature coefficient		-0.38 %/°C
Short circuit temperature Coefficient		3.5 mA/°C
Open circuit temperature Coefficient		-176.6 mV/°C
Nominal operating cell Temperature		-40°C to 85°C

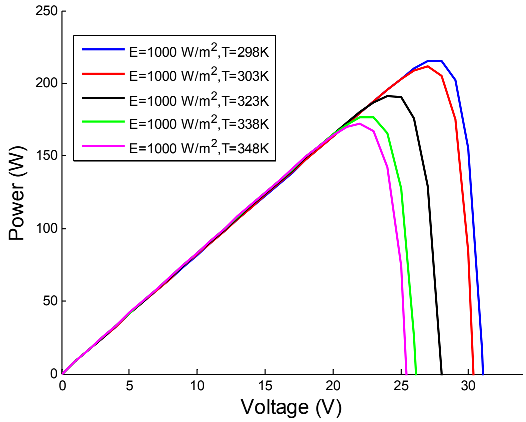

Fig. 7. P-V characteristics of PV cell with varing temperature profile

To illustrate the effect of temperature on the output voltage and output power of solar cell, temperature of the solar cell is varied from 298K to 343K keeping the solar irradiance constant at 1000 W/m^2. The plot of power-voltage with respect to temperature is shown in Fig. 7.

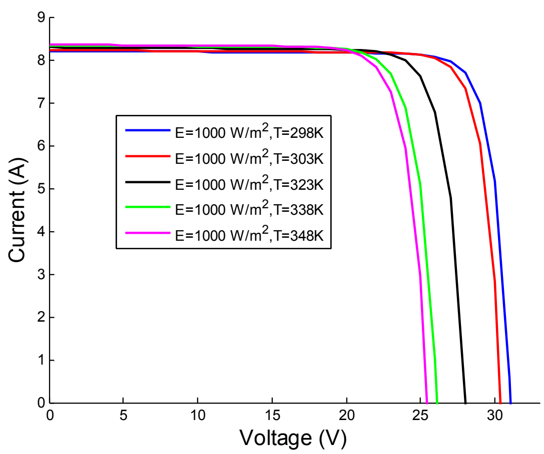

Fig. 8. I-V charactersitics of PV cell with varying temperature profile

The plot of voltage-current with respect to variable temperature is shown in Fig. 8.

Perturb and observe MPPT algorithm is used to provide necessary gate pulse to the MOSFETs of the synchronous buck converter. The design consideration of PV based battery charger is shown in Table II. The battery charger works in two distinct mode such as bulk charging mode and float charging mode. In bulk charging mode (when battery voltage is less than 13V), MPPT algorithm comes in to effect. When battery voltage is equal to the maximum battery voltage, float charging mode comes in to effect. The system is shut down when the power output of PV panel is less than 1 W.

TABLE II. SPECIFICATION OF SOLAR BATTERY CHARGER

	Parameters	Parameter	Values
Synchronous Buck Converter	Inductor	L	330 µH
	Capacitor	C	220 µF
	Switching frequency	f_{sw}	31 kHz
PV Module	Minimum wattage	$P_{\min}$	1 W
	Low wattage	P_{low}	5 W
Lead-Acid Battery	Maximum Voltage	V_{b_max}	14.1 V
	Minimum Voltage	V_{b_min}	11 V
	High Voltage	V_{b_h}	13 V

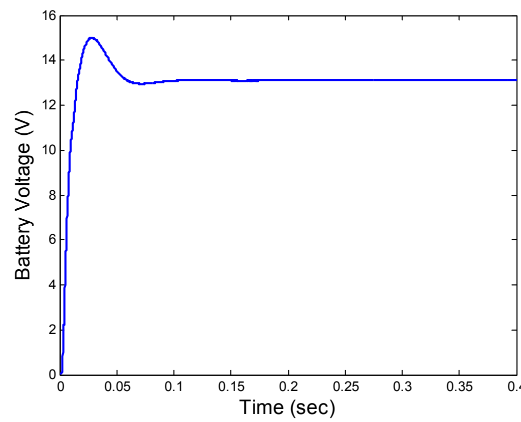

(a)

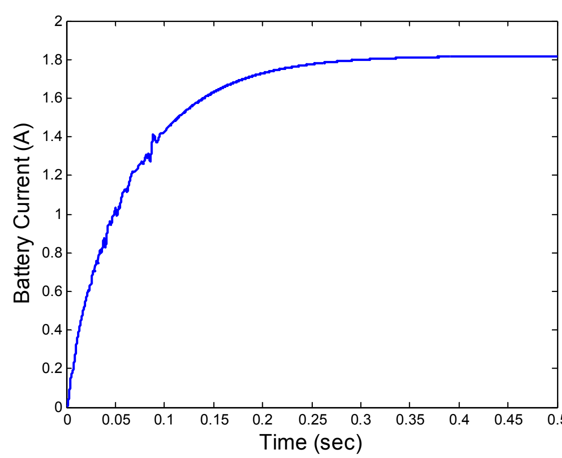

(b)

Fig. 9. (a) Battery voltage (b) battery current in normal condition (uniform irradiance)

Fig. 9(a) presents the battery voltage i.e 13.1 V DC and battery current i.e 1.8 A during uniform solar irradiance when bulk charging mode comes in to effect and the battery is charged using MPPT algorithm.

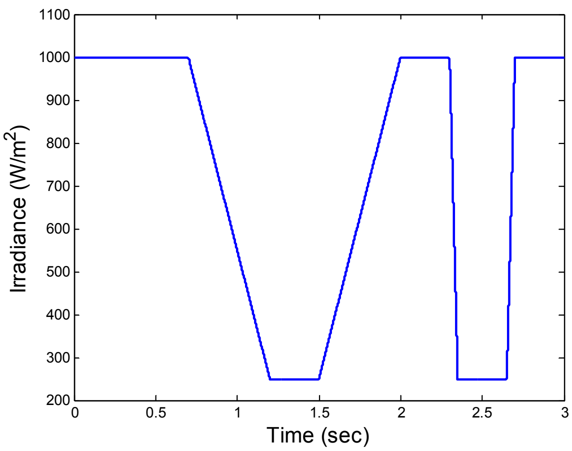

(a)

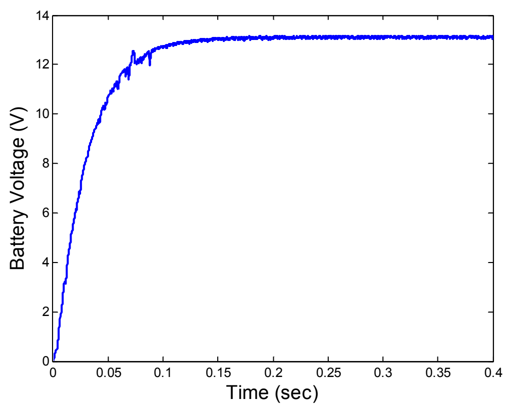

(b)

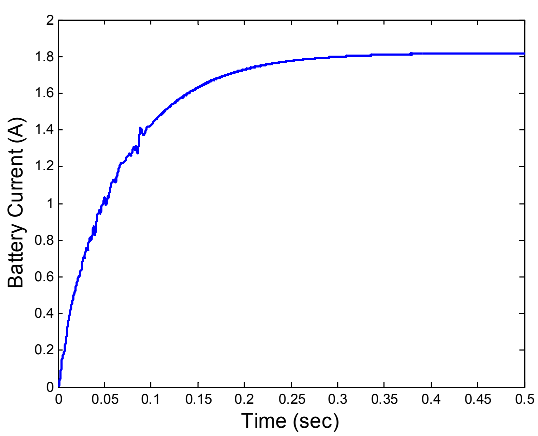

(c)

Fig. 10. (a) Variation in solar irradiance (b) battery voltage (c) battery current during variation in solar irradiance

Fig. 10(a) shows the variation in solar irradiance. Due to such variation, the output power of PV panel changes. In such condition, the PV charger provides the same charging capacity to the battery in bulk charging mode. Fig. 10(b) and Fig. 10(c) shows the respective battery voltage and battery current during change in solar irradiance condition.

VII. Conclusion

This paper provides a comprehensive design and implementation details of PV based lead acid battery charger system. The said technique charges the lead-acid battery either in bulk charging mode or in float charging mode. This technique is implemented with the help of PV panel, perturb and observe MPPT algorithm, synchronous buck converter and lead acid battery. Simulation results have validated the theoretical aspect of the concept.

References

[1] M. Yilmaz and P. T. Krein, "Review of battery charger topologies, charging power levels, and infrastructure for plug-in electric and hybrid vehicles," *IEEE Trans. Power Electron.*, vol. 28, no. 5, pp. 2151–2169, 2013.

[2] S. Ketsingsoi and Y. Kumsuwan, "An off-line battery charger based on buck-boost power factor correction converter for plug-in electric vehicles," *Energy Procedia*, vol. 56, pp. 659–666, 2014.

[3] S. Chiang, H.-J. Shieh, and M.-C. Chen, "Modeling and control of pv charger system with sepic converter," *IEEE Trans. Ind. Electron.*, vol. 56, no. 11, pp. 4344–4353, 2009.

[4] Thanh-Tan Nguyen, Hyung Won Kim, Geun Hing Lee, Woojin Choi, "Design and implementation of the low cost and fast solar charger with rooftop PV array of the vehicle," Solar Energy, 96, 2013, pp. 83-95.

[5] Shah Arifur Rahman, Rajiv K. Verma, Tim Vanderheide, "Generalized model of a photovoltaic panel," IET Renewable Power Generation, vol. 8, issue 3, 2014, pp. 217-229.

[6] Hadjer Bounechba, Aissa Bouzid, Hamza Snani, Abderrazak Lashab, "Real time simulation of MPPT algorithms for PV energy system," *Electrical power and energy systems*, 83, 2016, pp. 67-78.

[7] Ronn Raedani, Moin Hanif, "Design, testing and comparison of P&O, IC and VSSIR MPPT techniques," in *Proc. Int. Conf. Renewable Energy Research Application*, 2014, pp. 322-330.

[8] Aranzazu D. Martin, Jesus R. Vazquez, "MPPT algorithms comparision in PV systems: P&O, PI, neuro-fuzzy and backsteping controls," in Proc. IEEE Int. Conf. Industrial Technology, 2015, pp. 2841-2847.

[9] G.J. Kish, J.J. Lee, P.W. Lehn, "Moelling and control of photovoltaic panels utilizing the incremental conductance method for maximum power point tracking," *IET Renewable Power Generation*, vol. 6, issue 4, 2012, pp. 259-266.

[10] Yie-Tone Chen, Yi-Cheng Jhang, Ruey-Hsun Liang, "A fuzzy-logic based auto-scaling variable step-size MPPT method for PV systems," *Solar Energy*, vol. 126, 2016, pp. 53-63.

[11] Ziyad M. Salameh, Margaret A. Casacca, William A. Lynch, "A mathematical model for lead-acid batteies," *IEEE Trans. Energy Conversion*, vol. 7, no. 1, 1992, pp. 93-98.

[12] John P. Nelson, and William D. Bolin, "Basics and advances in battery systems," *IEEE Trans. Ind. Appl.*, vol. 31, no. 2, Mar/Apr 1995, pp. 419-428.